ELSEVIER

www.elsevier.nl/locate/jorganchem

Journal of Organometallic Chemistry 607 (2000) 208–212

Journal of Organometallic Chemistry

Trends in back-bonding in the series *trans*-[M(C≡CR)Cl(PH$_3$)$_4$] (M = Fe, Ru, Os; R = H, Ph, C$_6$H$_4$NO$_2$-4)

Christopher D. Delfs, Rob Stranger *, Mark G. Humphrey, Andrew M. McDonagh

Department of Chemistry, The Australian National University, Canberra ACT 0200, Australia

Received 17 April 2000; received in revised form 30 May 2000

Dedicated to Professor Martin Bennett on his 65th birthday, in recognition of his outstanding contributions to organometallic chemistry.

Abstract

The electronic structure of the complexes *trans*-[M(C≡CR)Cl(PH$_3$)$_4$] (M = Fe, Ru, Os; R = H, Ph, C$_6$H$_4$NO$_2$-4) has been investigated using approximate density functional theory in order to examine the M–C back-bonding interaction. For all three metal systems, the π back-bonding increases in the order R = H < Ph < C$_6$H$_4$-4-NO$_2$, indicating that the π acceptor character of the acetylide ligand increases with the electron-withdrawing ability of the substituent. The inclusion of relativistic effects in the calculations results in a metal dependence of Fe ~ Ru < Os for the back-bonding, consistent with the observed trend in quadratic hyperpolarizabilities, β. © 2000 Published by Elsevier Science S.A. All rights reserved.

Keywords: Metal–carbon backbonding; Density functional theory; Relativistic effects

1. Introduction

Organic and organometallic molecules containing a highly polarizable conjugated backbone with donor and acceptor groups attached at the termini, constituting asymmetric push–pull systems, have been studied extensively for their nonlinear optical (NLO) properties [1,2]. Synthetic strategies which have been suggested to maximize the NLO response of organometallics generally facilitate the mixing between metal and ligand-based orbitals, and include incorporation of the metal into the π system of the chromophore and introduction of some metal–carbon multiple bonding [3]. η^1-Alkynyl and vinylidene complexes satisfying these design criteria are therefore actively being investigated to determine their NLO properties [4–19].

In previous density functional studies [20], we found that, although the π back-bonding interaction in *trans*-[Ru(C≡CR)Cl(PH$_3$)$_4$] complexes was weak, the calculated trend reflected the π acceptor ability of the substituted acetylide ligand and that increasing back-bonding was correlated to increasing hyperpolarizability, β. The effect of metal variation upon back-bonding and NLO response is also of interest. In a series of (η^5-cyclopentadienyl)-metal complexes possessing *p*-substituted benzonitrile ligands, β was found to undergo a three-fold increase in proceeding from the Ru complex to the Fe homologue [2]. The larger value of β for the Fe complex was attributed to increased back-bonding, as it reflected the observed decrease in the ν(C≡N) stretching frequency on coordination of the metal which is greatest for the Fe complex. Recent studies on the hyperpolarizability of metal-η^1-alkynyl complexes, however, have shown no correlation between the hyperpolarizability, β, and the ν(C≡C) stretching frequency, both of which are considered to be indicators of M–C π back-bonding [21]. We have therefore undertaken calculations using approximate density functional theory on compounds with the general formula *trans*-[M(C≡CR)Cl(PH$_3$)$_4$] (M = Fe, Ru, Os; R = H, Ph, 4-C$_6$H$_4$NO$_2$) in order to explore the metal dependence of back-bonding in this series, the results of which are described herein.

* Corresponding author. Fax: +61-2-62490760.
E-mail address: rob.stranger@anu.edu.au (R. Stranger).

PII: S0022-328X(00)00349-1

2. Computational details

In the calculations described here we have followed the usual practice of simplifying the compounds to model complexes which are more amenable to calculation. Ligands such as 1,2-bis(methylphenylphosphino)benzene, dppe, PPh_3 and PMe_3 have been approximated using the appropriate number of PH_3 groups. These calculations have been performed with the Amsterdam Density Functional (ADF) program (versions 2.3.0 and 1999) [22,23] running on Linux/Pentium 600 MHz computers. The basis functions for all the main group elements are Slater functions of double zeta quality with an additional polarization function. For the transition metals triple zeta basis functions were employed. The 1s orbitals for C, N and O, all orbitals up to and including 2p for P and Cl, and all orbitals up to and including 3p, 4p and 4f for Fe, Ru and Os, respectively, were treated using the frozen core approximation. Calculations on compounds containing the C≡CH group were performed in C_{4v} symmetry but for comparative purposes, the results are given for C_{2v} symmetry. Calculations on compounds with the alkynyl ligands, C≡CPh and 4-C≡C$C_6H_4NO_2$ were performed in the C_{2v} point group but the $[MCl(PH_3)_4]$ fragment of the molecules was constrained to maintain C_{4v} symmetry. The local density functional, including exchange and correlation, of Vosko, Wilk and Nusair [24] and the gradient corrections of Becke [25] and Perdew [26] for the exchange and correlation, respectively, were used throughout. Geometry optimizations were performed using the method of Versluis and Ziegler [27–29]. Relativistic effects were included using the zeroth order regular approximations (ZORA) [30–32].

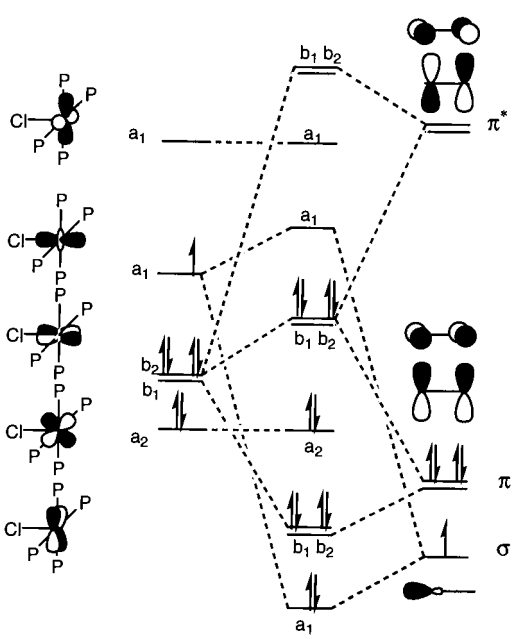

Fig. 1. Schematic representation of the molecular orbital (MO) diagram for *trans*-$[M(C{\equiv}CR)Cl(PH_3)_4]$.

3. Results and discussion

3.1. Geometries

The calculated molecular geometries are generally in good agreement with the available X-ray crystal structures [21], particularly in relation to the M–C and C≡C distances. The C≡C distances in the optimized structures for all the complexes in this study lie in the range 1.23–1.24 Å. The lack of sensitivity of the C≡C bond length to π back-donation from the metal center has been commented on previously [33]. In contrast, the M–C distances are notably shorter in all three metal systems when the acetylide substituent is C_6H_4-4-NO_2.

3.2. Analysis of back-bonding

The analysis of the M–C interaction was undertaken using the molecular fragment approach available in the ADF program and the bond energy decomposition scheme described by Ziegler and Rauk [34–37]. The partitioning of the molecule into two fragments allows the inspection of contributions to the metal–carbon bond in isolation [20,38]. The two molecular fragments are brought together without changing the relative positions of the atoms in each fragment and with the unpaired electrons in the orbitals participating in bond formation. In this procedure, the energy associated with the M–C interaction is separated into terms arising from the steric and orbital interactions:

$$\Delta E[\mathrm{M{-}C}] = \Delta E_{\mathrm{st}} + \Delta E_{\mathrm{oi}} + \Delta E_{\mathrm{corr}} \quad (1)$$

The ΔE_{st} term arises through a combination of electrostatic interactions between the two fragments and four-electron two-orbital repulsions. The term ΔE_{corr} corrects for the imperfect fit of the molecular density afforded by the auxiliary set of basis functions. The ΔE_{oi} term is a result of the two-electron two-orbital interactions which can be between two half filled orbitals or between a filled orbital on one fragment and a vacant orbital on the other. This term can be further subdivided into contributions from each of the irreducible representations of the relevant point group, in this case C_{2v} symmetry. Thus, Eq. (1) can be expanded to:

$$\Delta E[\mathrm{M{-}C}] = \Delta E_{\mathrm{st}} + \Delta E_{\mathrm{a_1}} + \Delta E_{\mathrm{a_2}} + \Delta E_{\mathrm{b_1}} + \Delta E_{\mathrm{b_2}} + \Delta E_{\mathrm{corr}} \quad (2)$$

A molecular orbital diagram showing the interaction between the $[MCl(PH_3)_4]^{\bullet}$ and $[C{\equiv}CR]^{\bullet}$ fragments is given in Fig. 1. Each fragment has a neutral charge and a single unpaired electron in the orbital that participates in the M–C σ bond.

Table 1
Components of the M–C bond energy (kJ mol^{-1}) for *trans*-$[M(C{\equiv}CR)Cl(PH_3)_4]$ [a,b]

Complex	ΔE_{st}	$\Delta E(a_1)$	$\Delta E(a_2)$	$\Delta E(b_1)$	$\Delta E(b_2)$	ΔE_{corr}	Bond energy
C≡CH							
Fe	531(514)	−1008(−987)	3(3)	−48(−46)	−48(−46)	(−2)	−571(−565)
No π*	531(514)	−1015(−994)	1(1)	−5(−4)	−5(−4)	(−2)	−493(−489)
Ru	561(514)	−1048(−990)	1(0)	−47(−42)	−47(42)	(−2)	−580(−562)
No π*	561(514)	−1057(−995)	0(0)	−4(−4)	−4(−4)	(−2)	−503(−491)
Os	803(515)	−1328(−1001)	0(1)	−57(−41)	−57(−41)	(3)	−640(−564)
No π*	803(515)	−1336(−1005)	0(0)	−7(−4)	−7(−4)	(3)	−549(−495)
C≡CPh							
Fe	519(512)	−992(−984)	2(3)	−53(−53)	−46(−46)	(−2)	−570(−566)
No π*	519(512)	−1000(−991)	1(2)	−5(−4)	−4(−4)	(1)	−489(−485)
Ru	560(534)	−1039(−1004)	0(1)	−53(−50)	−46(−44)	(3)	−577(−561)
No π*	560(534)	−1049(−1008)	0(0)	−4(−4)	−3(−44)	(0)	−495(−483)
Os	805(531)	−1324(−1013)	0(1)	−65(−48)	−56(−42)	(7)	−640(−563)
No π*	805(531)	−1333(−1016)	0(0)	−8(4)	−7(−4)	(5)	−543(−487)
$C{\equiv}CC_6H_4NO_2$							
Fe	543(526)	−1020(−1023)	2(3)	−69(69)	−52(−52)	(3)	−596(−613)
No π*	543(526)	−1029(−1029)	0(1)	−5(−6)	−5(5)	(1)	−495(−513)
Ru	584(524)	−1069(−1028)	0(0)	−66(−61)	−52(−48)	(3)	−603(−611)
No π*	584(524)	−1079(−1031)	0(0)	−4(−5)	−4(4)	(1)	−503(−518)
Os	853(480)	−1374(−1040)	−1(0)	−83(−59)	−65(−46)	(8)	−670(−656)
No π*	853(480)	−1384(−1041)	−1(0)	−9(−5)	−8(−4)	(5)	−548(−566)

[a] Non-relativistic values given in parentheses.
[b] ΔE_{corr} terms for relativistic calculations are negligible and therefore are not listed.

The alkynyl fragment, shown in Fig. 1 as $[C{\equiv}CH]^{\bullet}$, has a singly occupied sp-hybridized σ orbital, two filled π orbitals and two vacant π* orbitals at much higher energy. The orbital energy pattern for the $[MCl(PH_3)_4]^{\bullet}$ fragment is that expected for a metal ion in a C_{4v} symmetry, square pyramidal environment, namely a doubly occupied a_2 orbital, doubly occupied and degenerate b_1 and b_2 orbitals, a singly occupied a_1 orbital and a vacant a_1 orbital to highest energy. The b_1 and b_2 orbitals are degenerate as a consequence of the $[MCl(PH_3)_4]^{\bullet}$ fragment being forced to maintain C_{4v} symmetry. The singly occupied a_1 orbital is essentially a d_{z^2} orbital and its overlap with the sp-hybridized σ orbital of the $[C{\equiv}CH]^{\bullet}$ fragment forms the M–C σ bond. A vacant a_1 (σ*) orbital arises from the interaction between the metal $d_{x^2-y^2}$ orbital and the phosphine ligands. The t_{2g} orbitals split into a_2, b_1 and b_2 representations in C_{2v} symmetry with the a_2 orbital being non-bonding with respect to the M–C interaction. Since only the b_1 and b_2 orbitals can overlap with the alkynyl π and π* orbitals, we will refer to these as the dπ orbitals.

From the orbital interaction energies given in Table 1, it is immediately apparent that the energy associated with the σ (a_1) interaction between the metal and the carbon is much larger than that corresponding to the π ($b_1 + b_2$) interaction. This is consistent with results of calculations performed on the related system $[Fe(C{\equiv}CH)(L)_2(\eta\text{-}C_5H_5)]$ ($L = PH_3$, CO) [38]. Interaction between the dπ orbitals with the π orbitals of the alkynyl fragment (forward-bonding) destabilizes the dπ system relative to the non-bonding a_2 orbital. In contrast, interaction with the π* orbitals (back-bonding) leads to a relative stabilization of the dπ orbitals. Unfortunately, the forward-bonding and back-bonding contributions cannot be separated on symmetry grounds because the alkynyl π and π* orbitals have the same symmetry properties and both can overlap with the metal dπ orbitals. It is possible to discriminate between these two interactions, however, by removing the vacant π* orbitals which eliminates the dπ–π* contribution to the bond energy. This procedure is easily implemented within the ADF program through use of the *REMOVEFRAGORBITALS* key. The energy associated with the M–C back-bonding is then the difference between the $\Delta E(b_1)$ and $\Delta E(b_2)$ terms calculated with and without the alkynyl π* orbitals [20]. The residual $\Delta E(b_1)$ and $\Delta E(b_2)$ terms obtained form such a calculation would in principal reflect the forward bonding interaction. However, for the d^6 metal ions examined in this study, the dπ orbitals are filled and therefore the dπ–π interaction involves four-electron two-orbital repulsions which contribute mainly to the ΔE_{st} term in the energy decomposition scheme given by Eq. (2). A residual forward bonding interaction still appears in Table 1 as a result of the mixing of the dπ and π* orbitals. This has the effect of reducing the occupation of the dπ orbitals which in turn allows for some forward donation from the alkynyl π orbitals into the formally fully occupied metal dπ orbitals. Thus, the

calculated back-bonding energy in $[Fe(C{\equiv}CH)Cl(PH_3)_4]$ is -42 kJ mol^{-1} and the residual π forward-bonding energy is an order of magnitude smaller at -4 kJ mol^{-1}. The data in Table 1 indicates that overall the back bonding energy is relatively weak given that in all cases it is less than 10% of the M–C σ interaction. The lack of strong dπ–π* interactions between the metal and alkynyl fragments is the result of the π* orbitals of the alkynyl ligand being much higher in energy than the dπ orbitals of the metal fragment.

The variation in the back-bonding energy is plotted against the different ligands in Fig. 2. Only the results of the relativistic calculations are included here but similar trends are found for the non-relativistic calculations. In both cases, the trends are similar to previous calculations on the *trans*-$[Ru(C{\equiv}CR)Cl(PH_3)_4]$ series, which showed that the extent of π back-bonding

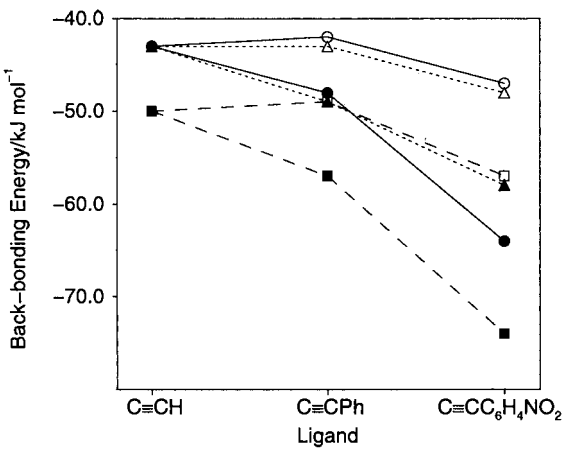

Fig. 2. Effect of varying the alkynyl ligand on back-bonding energies for *trans*-$[M(C{\equiv}CR)Cl(PH_3)_4]$. Calculations include relativistic corrections. ●, [$\Delta E(b_1)$, Fe], ○, [$\Delta E(b_2)$, Fe], ▲, [$\Delta E(b_1)$, Ru], △, [$\Delta E(b_2)$, Ru], ■, [$\Delta E(b_1)$, Os], □, [$\Delta E(b_2)$, Os].

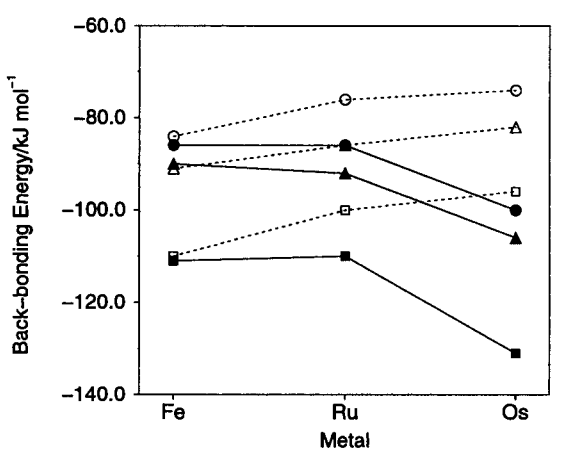

Fig. 3. Effect of varying the metal on back-bonding energies [$\Delta E(b_1) + \Delta E(b_2)$] for *trans*-$[M(C{\equiv}CR)Cl(PH_3)_4]$, with relativistic corrections (—) and without (···). ●/○, R = C≡CH, ▲/△, R = C≡CPh, ■/□, R = $C{\equiv}CC_6H_4$-4-NO_2.

reflected the π acceptor ability of the alkynyl group [20], i.e. the back-bonding energy follows the trend H < Ph < C_6H_4-4-NO_2. Thus, back-bonding is enhanced as the electron-withdrawing ability of the R substituent increases. It is important to note that in C_{2v} symmetry the π orbitals in C≡CPh and $C{\equiv}CC_6H_4$-4-NO_2 belong to two different irreducible representations, b_1 and b_2. In these calculations the phenyl ring is in the *yz* plane, and consequently the b_2 π system contains only the carbon p_y orbitals on the C≡C component of the alkynyl ligand. In contrast, the b_1 π system extends over both the C≡C and phenyl ring portions of the ligand and is therefore influenced to a much greater extent by π acceptor groups attached to the phenyl ring. This is clearly seen in Fig. 2 where the b_1 back-bonding energy is consistently larger than that calculated for b_2 when R = Ph, C_6H_4-4-NO_2.

The variation in the back-bonding energy with change in the metal is shown in Fig. 3. In the case of the non-relativistic calculations, the trend observed across all alkynyl ligands is Fe > Ru > Os. Although this trend is consistent with reported values of the IR stretching frequency ν(C≡C) [21], it is contrary to expectations for normal metal–ligand bonding interactions. The dπ orbitals of osmium are expected to be higher in energy than those of iron and hence have a stronger interaction with the π* orbitals of the alkynyl ligand, in turn leading to stronger back-bonding. However, it has been pointed out that the IR stretching frequency ν(C≡C) in terminal acetylenes is approximately 100 cm^{-1} lower than ν(C≡C) in internal acetylenes, as a result of coupling between the C≡C and C–H stretching vibrations [39,40]. Therefore, changes in the ν(C≡C) frequency may not necessarily be a good indication of ligand to metal back donation.

Although the inclusion of relativistic terms does not alter the trend in the back-bonding energy on varying the R group of the alkynyl ligand, it clearly has a large effect on the trend in back-bonding energy on varying the metal, as is evident from Fig. 3. With the relativistic corrections included, the back-bonding energy varies in the order Os > Ru ~ Fe. This trend can be explained qualitatively in terms of the energy separation between the metal dπ and alkynyl π* orbitals. Relativistic effects, which are known to stabilize s orbitals and destabilize d orbitals, are expected to be negligible for iron, small for ruthenium and large for osmium. The resultant large destabilization of the osmium dπ orbitals brings them closer in energy to the alkynyl π* orbitals, in turn increasing the interactions between these orbitals and thus the back-bonding energy. This trend in the back-bonding energy contrasts with the observed trend in ν(C≡C) but, as noted above, the latter may not be an accurate indication of π back-donation. However, the calculated trend with relativistic corrections included appears to reflect the observed trend in

quadratic hyperpolarizability, as measured by hyper-Rayleigh scattering [21].

4. Conclusions

The back-bonding interaction between the metal and the alkynyl ligand in the series *trans*-[M(C≡CR)-$Cl(PH_3)_4$] (M = Fe, Ru, Os; R = H, Ph, $C_6H_4NO_2$-4) is small relative to the M–C σ interaction. For all three metal systems, the π back-bonding in the complexes increases in the order R = H < Ph < C_6H_4-4-NO_2. Calculations performed without relativistic effects show a trend in the back-bonding energy that is somewhat counterintuitive, that is Fe > Ru > Os. Although this trend is consistent with the observed ν(C≡C) frequencies, it is contrary to expectations based on metal–ligand bonding where the 5d orbitals of Os should lie closer in energy to the π* orbitals of the alkynyl ligand than those of Fe, in turn leading to greater back bonding. When relativistic effects are included, the opposite trend, Os > Ru ~ Fe, is found, in agreement with the observed trend in quadratic hyperpolarizabilities.

References

[1] P.N. Prasad, D.J. Williams, Introduction to Nonlinear Optical Effects in Molecules and Polymers, Wiley, New York, 1991.
[2] W. Wenseleers, A.W. Gerbrandij, E. Goovaerts, M.H. Garcia, M.P. Robalo, P.J. Mendes, J.C. Rodrigues, A.R. Dias, J. Mater. Chem. 8 (1998) 925.
[3] J.C. Calabrese, L.T. Cheng, J.C. Green, S.R. Marder, W. Tam, J. Am. Chem. Soc. 113 (1991) 7227.
[4] A.M. McDonagh, I.R. Whittall, M.G. Humphrey, D.C.R. Hockless, B.W. Skelton, A.H. White, J. Organomet. Chem. 523 (1996) 33.
[5] A.M. McDonagh, I.R. Whittall, M.G. Humphrey, B.W. Skelton, A.H. White, J. Organomet. Chem. 519 (1996) 229.
[6] A.M. McDonagh, M.P. Cifuentes, I.R. Whittall, M.G. Humphrey, M. Samoc, B. Luther-Davies, D.C.R. Hockless, J. Organomet. Chem. 526 (1996) 99.
[7] I.R. Whittall, A.M. McDonagh, M.G. Humphrey, M. Samoc, Adv. Organomet. Chem. 43 (1999) 349.
[8] I.R. Whittall, M.P. Cifuentes, M.J. Costigan, M.G. Humphrey, S.C. Goh, B.W. Skelton, A.H. White, J. Organomet. Chem. 471 (1994) 193.
[9] I.R. Whittall, M.G. Humphrey, D.C.R. Hockless, B.W. Skelton, A.H. White, Organometallics 14 (1995) 3970.
[10] I.R. Whittall, M.G. Humphrey, M. Samoc, J. Swiatkiewicz, B. Luther-Davies, Organometallics 14 (1995) 5493.
[11] I.R. Whittall, M.G. Humphrey, A. Persoons, S. Houbrechts, Organometallics 15 (1996) 1935.
[12] I.R. Whittall, M.G. Humphrey, S. Houbrechts, A. Persoons, D.C.R. Hockless, Organometallics 15 (1996) 5738.
[13] I.R. Whittall, M.G. Humphrey, M. Samoc, B. Luther-Davies, Angew. Chem. Int. Ed. Engl. 36 (1997) 370.
[14] I.R. Whittall, M.P. Cifuentes, M.G. Humphrey, B. Luther-Davies, M. Samoc, S. Houbrechts, A. Persoons, G.A. Heath, D. Bogsanyi, Organometallics 16 (1997) 2631.
[15] I.R. Whittall, M.G. Humphrey, S. Houbrechts, J. Maes, A. Persoons, S. Schmid, D.C.R. Hockless, J. Organomet. Chem. 544 (1997) 277.
[16] I.R. Whittall, M.G. Humphrey, M. Samoc, B. Luther-Davies, D.C.R. Hockless, J. Organomet. Chem. 544 (1997) 189.
[17] I.R. Whittall, M.G. Humphrey, D.C.R. Hockless, Aust. J. Chem. 50 (1997) 991.
[18] I.R. Whittall, M.P. Cifuentes, M.G. Humphrey, B. Luther-Davies, M. Samoc, S. Houbrechts, A. Persoons, G.A. Heath, D.C.R. Hockless, J. Organomet. Chem. 549 (1997) 127.
[19] I.R. Whittall, M.G. Humphrey, D.C.R. Hockless, Aust. J. Chem. 51 (1998) 219.
[20] J.E. McGrady, T. Lovell, R. Stranger, M.G. Humphrey, Organometallics 16 (1997) 4004.
[21] A.M. McDonagh, Transition Metal Acetylide Complexes for Non-Linear Optics, Ph.D. Thesis, The Australian National University, Australia, 1999.
[22] E.J. Baerends, A Bérces, C. Bo, P.M. Boerrigter, L. Cavallo, L. Deng, R.M. Dickson, D.E. Ellis, L. Fan, T.H. Fischer, C. Fonseca Guerra, S.J.A. van Gisbergen, J.A. Groeneveld, O.V. Gritsenko, F.E. Harris, P. van den Hoek, H. Jacobsen, G. van Kessel, F. Kootstra, E. van Lenthe, V.P. Osinga, P.H.T. Philipsen, D. Post, C. Pye, W. Ravenek, P. Ros, P.R.T. Schipper, G. Schreckenbach, J.G. Snijders, M. Sola, D. Swerhone, G. te Velde, P. Vernooijs, L. Versluis, O. Visser, E. van Wezenbeek, G. Wiesenekker, S.K. Wolff, T.K. Woo, T. Ziegler, Amsterdam Density Functional, 1999.
[23] C. Fonseca Guerra, J.G. Snijders, G. te Velde, E.J. Baerends, Theor. Chem. Acc. 99 (1998) 391.
[24] S.H. Vosko, L. Wilk, M. Nusair, Can. J. Phys. 58 (1980) 1200.
[25] A.D. Becke, Phys. Rev. A 38 (1988) 3098.
[26] J.P. Perdew, Phys. Rev. B 33 (1986) 8822.
[27] T.H. Fischer, J. Almlof, J. Phys. Chem. 96 (1992) 9768.
[28] L. Fan, T. Ziegler, J. Chem. Phys. 95 (1991) 7401.
[29] L. Versluis, T.J. Ziegler, J. Chem. Phys. 88 (1988) 322.
[30] T. Ziegler, V. Tschinke, E.J. Baerends, J.G. Snijders, J. Phys. Chem. 93 (1989) 3050.
[31] E. van Lenthe, E.J. Baerends, J.G. Snijders, J. Chem. Phys. 99 (1993) 4597.
[32] J.G. Snijders, E.J. Baerends, P. Ros, Mol. Phys. 38 (1979) 1909.
[33] J. Manna, K.D. John, M.D. Hopkins, Adv. Organomet. Chem. 38 (1995) 79.
[34] T. Ziegler, A. Rauk, Theor. Chim. Acta 46 (1977) 1.
[35] T. Ziegler, A. Rauk, Inorg. Chem. 18 (1979) 1755.
[36] T. Ziegler, in: D.R. Salahub, N. Russo (Eds.), Metal–Ligand Interactions: from atoms to clusters to surfaces, Kluwer, Dordrecht, 1992, p. 367.
[37] T. Ziegler, A. Rauk, Inorg. Chem. 18 (1979) 1558.
[38] N.M. Kostic, R.F. Fenske, Organometallics 1 (1982) 974.
[39] D.L. Lichtenberger, S.K. Renshaw, R.M. Bullock, J. Am. Chem. Soc. 115 (1993) 3276.
[40] J. Dale, Chemistry of Acetylenes, Marcel Decker, New York, 1969.